Etch Damage of Ge$_2$Sb$_2$Te$_5$ for Different Halogen Gases

Se-Koo Kang[1], Min-Hwan Jeon[1], Jong-Yoon Park[1], Myung S. Jhon[2], and Geun-Young Yeom[1,3]*

[1]SKKU Advanced Institute of Nano Technology (SAINT), Sungkyunkwan University, Suwon, Gyeonggi 440-746, Korea
[2]Department of Chemical Engineering, Carnegie Mellon University, Pittsburgh, PA 15213, U.S.A.
[3]Department of Advanced Materials Science and Engineering, Sungkyunkwan University, Suwon, Gyeonggi 440-746, Korea

Etch damage of Ge$_2$Sb$_2$Te$_5$ (GST) has been investigated after etching in halogen inductively coupled plasmas (ICPs) such as CF$_4$, Cl$_2$, and HBr. X-ray photoelectron spectra of Ge, Sb, and Te on the etched surfaces showed different depths of etch damage depending on the halogen-based plasmas. The blank GST etched by CF$_4$ showed a lower total-halogen-percentage remaining on the etched surface than that etched by Cl$_2$ even though the depth of halogenations was the deepest for the GST etched by CF$_4$ owing to the highest reactivity. However, when a GST feature masked by SiO$_2$/Ti/TiN was etched, owing to the reaction of O from the SiO$_2$ mask and C from CF$_4$, a thinner/or no C–F polymer appeared to be formed on the etched sidewall; therefore, the highest halogenation was observed on the GST etched by CF$_4$. Among the halogen-gases investigated, HBr showed the lowest damage due to the lowest reactivity. © 2011 The Japan Society of Applied Physics

1. Introduction

Phase change memory (PCM) technology is currently one of the intense R&D subjects by some companies and is one of the promising alternatives to the next-generation non-volatile memory (NVM), flash memory technologies, etc.[1–3] Most current PCM device study is focused on Ge$_2$Sb$_2$Te$_5$ (GST), but studies have been reported[4] on other chalcogenide-based phase-change materials such as GeTeAsSi, GeTe, GeSbTe, GeBiTe, GeSb(Cu, Ag), GeTeAs, InTe, AsSbTe, SeSbTe, and PbGeSb, even though the understanding of the chemical state and etch characteristic of the chalcogenide-based materials is incomplete.

Ge–Sb–Te based materials are known to be halogenated easily and apt to be damaged when exposed to halogen-gas-based plasmas in the etch process, whereas a stoichiometric composition of GST needs to be maintained for high-speed phase-change transformation and high a degree of cyclability. In particular, it is difficult to conserve the etched sidewall composition of GST without halogenation-induced degradation.

In a previous study, we investigated the degree of surface damage of GST etching with fluorocarbon plasmas and focused on the degree of sidewall damage after etching with different F/C ratio gases by using a topological X-ray photoelectron spectroscopic (XPS) study.[5] We demonstrated that less damaged etching can be performed with a lower F/C ratio fluorocarbon gas owing to the thicker C–F polymer formed on the GST surface and sidewalls during the etching, which protects against the diffusion of fluorine radicals to the GST film. In this article, the etching of GST with three types of halogen gas is described and the extent of the surface damage of GST during the etching by different halogen-gas-based inductively coupled plasmas (ICPs) such as CF$_4$, Cl$_2$, and HBr is investigated.

2. Experimental Methods

The etching system used in this study was an 8-in. diameter inductively coupled plasma system (STS PLC) and a schematic diagram of the etch system is shown in Fig. 1. The ICP chamber wall was made of a ceramic cylinder and the ICP antenna made of 1-turn copper coil was wound around the ceramic wall. 13.56 MHz rf power was applied
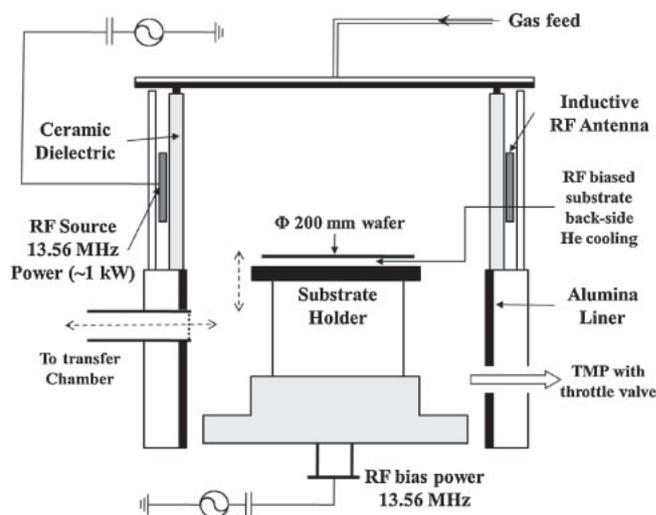

Fig. 1. Schematic diagram of the ICP etch system used in this study.

to the ICP source and the substrate was also rf biased by applying a separate 13.56 MHz rf power. The 100-nm-thick GST samples were prepared on SiO$_2$/Si substrates by rf magnetron co-sputtering from GeTe and Sb$_2$Te$_3$ targets and some of the samples were patterned with an SiO$_2$ hard mask after depositing a Ti (as an adhesion layer of 5 nm)/TiN layer on the GST films similarly to those described in our previous article.[5] The composition of the sputter-deposited GST was known to be Ge : Sb : Te = 22 : 22 : 56 (XPS analysis showed that the actual composition was Ge : Sb : Te = 26 : 26 : 48). The etch depth was measured using a surface profilometer (Tencor Alpha-step 500). The chemical bonding characteristics of the blank GST film surface and the sidewall of the patterned GST film after the etching were examined by XPS (VG Microtech ESCA2000) using an Al Kα twin-anode source with a photon energy of 1486.6 eV. The XPS spectra were deconvoluted using a least squares fitting technique by the Avantage fitting program supplied by VG Microetch. The etch profiles of the patterned GST samples were examined by field-emission scanning electron microscopy (FE-SEM; Hitachi S-4700).

3. Results and Discussion

The etch rates of GST by CF$_4$, Cl$_2$, and HBr ICPs were
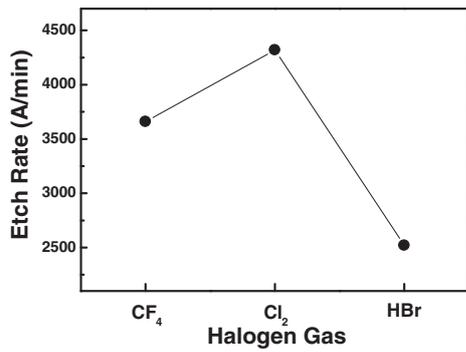
*E-mail address: gyyeom@skku.edu

Fig. 2. Etch rates of $Ge_2Sb_2Te_5$ by ICP etching as a function of different halogen-based gases.

Table I. Boiling points of the GST-halogen compounds.[6,7]

		Ge		Sb		Te	
		Bonding	b.p. (°C)	Bonding	b.p. (°C)	Bonding	b.p. (°C)
F		GeF_4	−36.5	SbF_5	141	TeF_4	196
		GeF_2	130	SbF_3	345	TeF_6	−39
Cl		$GeCl_4$	86.6	$SbCl_3$	220	$TeCl_2$	328
		$GeCl_2$	↑	$SbCl_5$	140	$[TeCl_4]_4$	387
Br		$GeBr_4$	186	$SbBr_3$	286	$TeBr_2$	339
		$GeBr_2$	150			$[TeBr_4]_4$	414

b.p.: boiling point

observed at the condition of an rf inductive power of 500 W and a bias voltage of −100 V while sustaining the gas flow rate of each halogen gas and the process pressure at 50 sccm and 3 mTorr, respectively. The result is shown in Fig. 2 and, as shown in the figure, the Cl_2 plasma showed the highest etch rate of GST by showing about 432 nm/min while the CF_4 plasma and the HBr plasma showed etch rates of 366 and 252 nm/min, respectively. Table I shows the boiling point of halogen compounds of Ge, Sb, and Te at STP (standard temperature and pressure; 1 atm, 25 °C) state.[6,7] As shown in Table I, the halides of Ge, Sb, and Te showed higher vapor pressures in the halogen gas sequence of F > Cl > Br. On the other hand, in Fig. 2, the GST etched by CF_4 plasma showed a lower etch rate than that etched by Cl_2, possibly owing to the formation of a thin C–F polymer for the CF_4 plasma, which prevents the etching of GST.

Figure 3 shows the XPS binding peak spectra of Ge, Sb, and Te after Ar^+ ion depth profiling of the blank GST films etched by CF_4, Cl_2, and HBr ICPs. The ion-gun energy and ion current of the XPS Ar^+ ion gun were set to 2 kV and

2 μA, respectively. The etch depth of GST by the CF_4, Cl_2, and HBr ICPs was kept at about 50 nm. The Ge 2p peak was separated into halogenated peaks such as peaks at 1219.5 eV (Ge^b) from Ge–F_x, at 1219.7 eV (Ge^c) from Ge–Cl_x, and at 1218.5 eV (Ge^d) from Ge–Br_x in addition to the metallic binding peak of Ge–Te located at 1217.6 eV (Ge^a). In the case of Sb $3d_{5/2}$, in addition to the peak at 528.7 eV (Sb^a) due to the metallic homopolar bonding of Sb–Te[8] (according to the article, Sb has a binding energy of 528.9 eV, which is very close to those we observed in the experiment within a tenth of eV), the peaks related to Sb-halides at 530.8 eV (Sb^b) from Sb–F_x, 531.7 eV (Sb^c) (possibly also related to the oxidation) and 529.5 eV (Sb^d) from Sb–Cl_x, and 529.3 eV (Sb^e) from Sb–Br_x could be observed. In fact, the peaks from Sb^b–Sb^e appear to be more related to the mixture of halide bonding and metallic bonding because these peak locations are changed continuously with the depth profiling. For the Te $3d_{5/2}$, the peak related to the metallic bonding was observed at 573.1 eV (Te^e) for HBr ICP (metallic homopolar binding energy of Te $3d_{5/2}$ is known to be at 573.1 eV for Te–Te bonding and 572.5 eV for Te–Ge bonding[9–13]) while other peaks at 573.9 eV (Te^a) and 573.5 eV (Te^c) for CF_4 and Cl_2 ICP, respectively, are
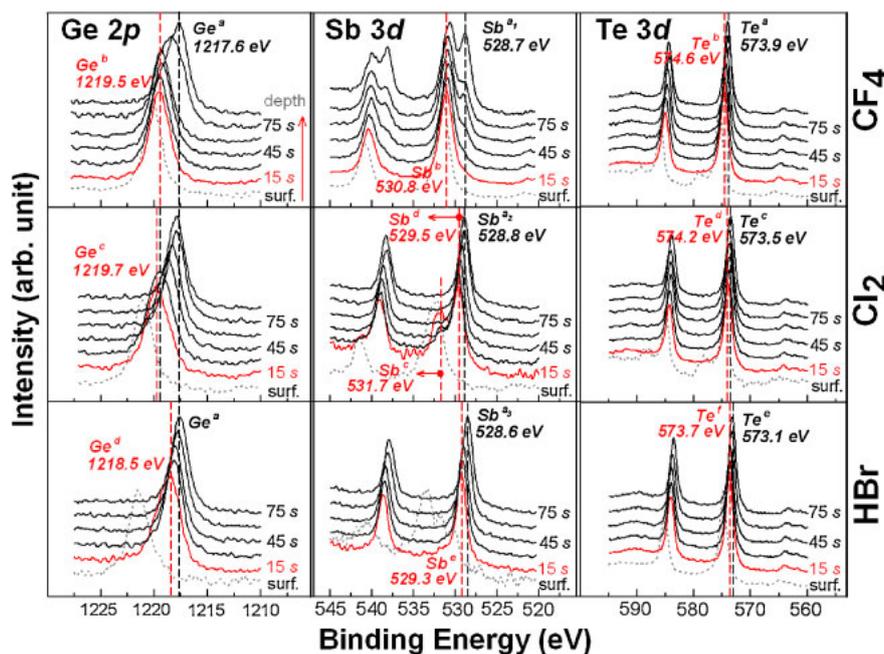

Fig. 3. (Color online) XPS spectra of each component of the GST films after the etching in CF_4, Cl_2, and HBr ICPs as a function of the sputter time during the Ar^+ ion depth profiling.

Table II. Atomic percent of GST and halogen components on the blank GST surface etched by various halogen gases (XPS data of F 1s, Cl 2p, and Br 3d were taken after sputtering for 15 s with Ar^+ ions).

	CF_4	Cl_2	HBr
Halogen[a]	17.07	17.79	16.70
Ge	23.51	13.57	16.55
Sb	26.77	16.16	17.58
Te	32.65	52.48	49.17

a) (F, Cl, Br)

related to the mixture of metallic bonding and halide bonding. Also, the peaks observed at 574.6 eV (Te[b]), 574.2 eV (Te[d]), and 573.7 eV (Te[f]) are also related to the Te-halide or the mixture of metallic bonding and halide bonding for CF_4, Cl_2, and HBr, respectively.

As shown in Fig. 3, for CF_4-etched GST, even after the sputtering for 75 s, the halide appears to remain in the GST while the GST etched by Cl_2 and HBr appears to be removed completely around 75 s and before 75 s of sputtering, respectively. The deeper halide formation of GST in the sequence of $CF_4 > Cl_2 >$ HBr is believed to be related to the strength of the chemical bond in diatomic molecules (kJ/mol) as shown below:[6]

$$F\text{–}Ge\ (485 \pm 21) > Cl\text{–}Ge\ (\sim 431)$$
$$> Ge\text{–}Te\ (340 \pm 14.6) > Br\text{–}Ge\ (255 \pm 29), \quad (1)$$
$$F\text{–}Sb\ (439 \pm 96) > Cl\text{–}Sb\ (360 \pm 50)$$
$$> Br\text{–}Sb\ (314 \pm 59) > Sb\text{–}Te\ (299.2 \pm 6.3). \quad (2)$$

In the case of Te-halides, no published data could be obtained; however, a similar trend is expected. Therefore, due to the higher reactivity of GST in the sequence of F > Cl > Br, the GST surface is believed to be more damaged by forming deeper halides on the GST surface during the etching in the sequence of $CF_4 > Cl_2 >$ HBr. On the other hand, as shown in Fig. 3, owing to the formation of a teflon-like C–F polymer layer on the GST surface during the etching by CF_4 plasma, the damage (that is, the degree of halide formation) of the top-most surface area (up to 15 s sputter depth of GST) appears to be lowest for the etching by CF_4 plasma as can be seen with the depth profile spectra of Ge 2p and Sb 3d.

The atomic percentages of the components in the etched GST were measured and the result is shown in Table II. The XPS data of F 1s, Cl 2p, and Br 3d were taken after sputtering for 15 s with Ar^+ ions to remove possible surface contamination during the air transfer to the XPS system after etching. As shown in the table, the percentage of GST has changed after the etching by halogen gases, especially for CF_4, by showing a significantly Te-deficient film (or Ge- and Sb-rich film). However, in the case of GST etched by Cl_2 and HBr, a slightly Te-rich film could be observed. The halogen percentages in the GST films were 17.07, 17.79, and 16.7% after the etching by CF_4, Cl_2, and HBr ICPs, respectively. Therefore, the GST etched by HBr ICP showed the lowest halogen content even though the differences are not significant. Each halogen XPS peak could be deconvoluted to free halogen in the film and halogen combined with GST and the result is shown in Fig. 4. The F 1s peak was deconvoluted to fluoride (fluorinated GST portion) at 686.0 eV and free F at 684.9 eV, Cl 2p into chloride (chlorinated GST portion) at 200.2 eV and free Cl at 198.5,
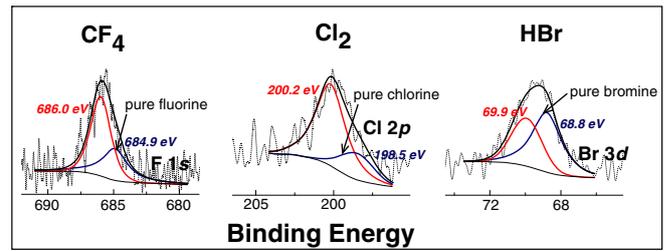

Fig. 4. (Color online) Halogen XPS peak in the blank GST thin film after the etching in CF_4, Cl_2, and HBr ICPs. XPS data of F 1s, Cl 2p, and Br 3d were taken after sputtering for 15 s with Ar^+ ions to remove possible surface contamination during the air transfer to the XPS system after etching.
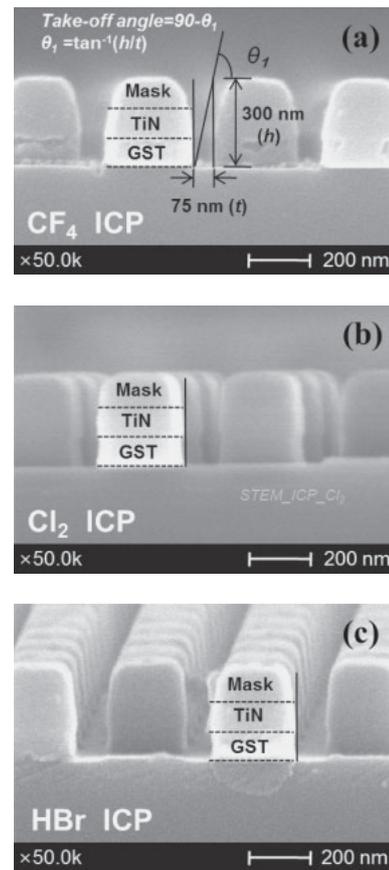

Fig. 5. Cross-sectional SEM images of the etched GST samples.

and Br 3d into bromide at 69.9 eV and free Br at 68.8 eV. When the peaks were deconvoluted, the percentages of halogen combined with GST etched by CF_4, Cl_2, and HBr ICPs were estimated to be 12.12, 13.53, and 7.02%, respectively; therefore, the GST etched by HBr ICP also showed the lowest halogenation. In Table II and Fig. 4, a lower halogen percentage and lower halogenation were observed for the GST etched by CF_4 ICP than for that etched by Cl_2 ICP even though the halogenated depth appeared to be the deepest for the CF_4-etched GST, as shown in Fig. 3. The lower halogen percentage and lower halogenations of the CF_4-etched GST than of the GST etched by Cl_2 ICP appear to be related to the C–F polymer formed on the GST surface for the CF_4-etched GST.
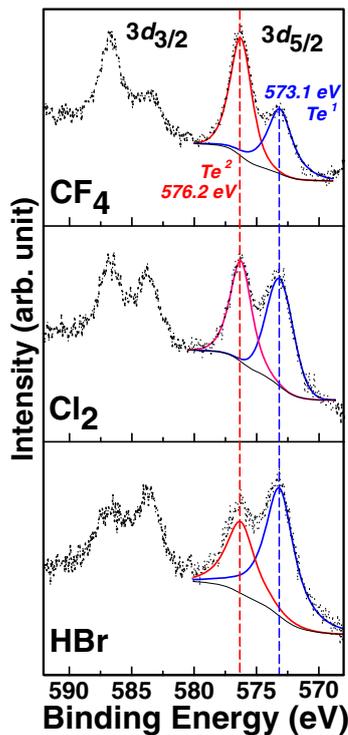
Fig. 6. (Color online) XPS spectra of Te 3d in the patterned GST sidewall etched with different halogen gases in an ICP etching system.

The GST masked with patterned $SiO_2/Ti/TiN$ was etched by CF_4, Cl_2, and HBr ICPs and the results are shown in Figs. 5(a)–5(c), respectively. As shown in the figures, the GST etched by CF_4, Cl_2, and HBr ICPs showed near vertical profiles. The sidewall of GST was examined by XPS analysis at a tilted angle as shown in Fig. 5 to investigate the sidewall damage of the GST features during the etching of GST by halogen gases and the result is shown in Fig. 6 for Te $3d_{5/2}$ (due to the lower signals for XPS peaks related to Ge and Sb, only the Te peak is shown). The Te $3d_{5/2}$ peaks were fitted into two components whose positions are related to metallic bonding at 573.1 eV (Te^1) and Te-halide near 576.4 eV (Te^2). The calculated intensity ratios of $Te^2/(Te^1 + Te^2)$ after the etching in CF_4, Cl_2, and HBr were 0.59, 0.44, and 0.33, respectively. Therefore, similar to the XPS data of the etched blank GST thin films, the GST etched by HBr showed the lowest halide on the sidewall of the etched GST feature. However, for the patterned GST, the CF_4-etched GST shows a higher halide on the sidewall than the Cl_2-etched GST. This is possibly due to a thinner/or no C–F polymer formation on the sidewall feature of GST by the reaction of C of CF_4 and O of SiO_2.

4. Conclusions

In summary, GST has been etched using various halogen gases such as CF_4, Cl_2, and HBr in an ICP system and the effect of halogen gas on the damage of the etched GST was investigated. The GST etched by Cl_2 showed the highest etch rate while that etched by HBr showed the lowest etch rate. The etch rate was related to the vapor pressure of

the halides of Ge, Sb, and Te, which showed higher vapor pressures in the halogen gas sequence of F > Cl > Br. However, the lower GST etch rate by CF_4 than that by Cl_2 appeared to be related to the formation of a C–F polymer on the GST surface for the CF_4-etched GST. Owing to the formation of the C–F polymer on the CF_4-etched GST, the total halogen percentage in the GST film was also lower for the GST etched by CF_4 ICP than that etched by Cl_2 ICP even though the depth of the halogenide appears to be deepest for the CF_4-etched GST owing to highest reactivity of F with GST. When the GST thin film masked by $SiO_2/Ti/TiN$ was etched using the halogen gases, the sidewall of the etched GST showed the highest degree of halogenation for CF_4 ICP compared with that etched by Cl_2 ICP owing to the thinner/ or no C–F polymer formation on the sidewall of the etched GST during the etching of GST by the reaction of O from SiO_2 and C from CF_4. Among the halogen gases investigated, HBr showed the lowest halogenide during the etching not only on the blank GST but also on the patterned GST owing to the lowest reactivity of GST with Br among the halogen gases investigated.

1) M. H. R. Lankhorst, B. W. S. M. M. Ketelaars, and R. A. M. Wolters: Nat. Mater. **4** (2005) 347.
2) J. E. Brewer and M. Gill: *Nonvolatile Memory Technologies with Emphasis on Flash* (IEEE Press, Piscataway, NJ, 2008).
3) K. Nakayama, K. Kojima, Y. Imai, T. Kasai, S. Fukushima, A. Kitagawa, M. Kakimoto, Y. Kakimoto, and M. Suzuki: Jpn. J. Appl. Phys. **42** (2003) 404.
4) T. Zhang, B. Liu, J.-L. Xia, Z.-T. Song, S.-L. Feng, and B. Chen: Chinese Phys. Lett. **21** (2004) 741.
5) S.-K. Kang, J. S. Oh, B. J. Park, S. W. Kim, J. T. Lim, G. Y. Yeom, C. J. Kang, and G. J. Min: Appl. Phys. Lett. **93** (2008) 043126.
6) D. R. Lide: *Handbook of Chemistry and Physics* (CRC Press, Boca Raton, FL, 2004) 84th ed.
7) Physical properties of halogen compounds on the Internet: Information about vapor pressure of halogen compounds. Retrieved June 2, 2010 from World Wide Web [http://www.webelements.com/].
8) J. González-Hernández, P. Herrera-Fierro, B. Chao, Y. Kovalenko, E. Morales-Sánchez, and E. Prokhorov: Thin Solid Films **503** (2006) 13.
9) C. D. Wagner, L. E. Davis, M. V. Zeller, J. A. Taylor, R. H. Raymond, and L. H. Gale: Surf. Interface Anal. **3** (1981) 211.
10) Binding energies of the GST compound on the Internet: NIST X-ray photoelectron spectroscopic database. Retrieved June 17, 2010 from World Wide Web [http://srdata.nist.gov/xps/].
11) Binding energies of the GST compound on the Internet: XPS chemical bond database. Retrieved June 17, 2010 from World Wide Web [http://www.lasurface.com/xps/index.php].
12) A. Thompson, I. Lindau, D. Attwood, P. Pianetta, E. Gullikson, A. Robinson, M. Howells, J. Scofield, K.-J. Kim, J. Underwood, J. Kirz, D. Vaughan, J. Kortright, G. Williams, and H. Winick: *X-ray Data Booklet* (Lawrence Berkeley National Laboratory, Berkeley, CA, 2001) 2nd ed.
13) J. F. Moulder, W. F. Stickle, P. E. Sobol, and K. D. Bomben: *Handbook of X-ray Photoelectron Spectroscopy* (Perkin-Elmer, Eden Prairie, MN, 1992).